

Dissociative Adsorption of Water on Ge(100)-(2 × 1): First-Principles Theory

Andrew Föraker and Douglas J. Doren*

Department of Chemistry and Biochemistry, University of Delaware, Newark, Delaware 19716

Received: December 16, 2002; In Final Form: April 30, 2003

A first-principles study of the dissociative adsorption of water on Ge(100)-(2 × 1) is described, on the basis of density functional theory with a cluster model of the surface. Experiments have shown that water incident on the Ge(100)-(2 × 1) surface has a very small probability of dissociative adsorption, indicating the presence of an activation barrier. This is in contrast to the analogous reaction on Si(100)-(2 × 1), which is unactivated. This difference is reproduced in the calculations, demonstrating the predictive capability of the methods used, though some caveats about basis sets are necessary. A frontier orbital analysis is used to identify the interactions that determine the transition state energy and underlie the difference between reactivity on Si and Ge.

Introduction

The reaction of water with the Si(100) surface in ultrahigh vacuum conditions has been widely studied, both as a prototype of semiconductor surface reactions and as a technologically useful reaction for growth of silicon dioxide layers (for a review of experimental work, see ref 1 and references therein). The closely analogous reaction on Ge(100) has not received as much attention, though it presents a paradox in our understanding of reactions on these surfaces. Both Si(100) and Ge(100) exhibit 2 × 1 reconstructions with similar buckled surface dimers, yet the dissociative adsorption of water on Si(100) proceeds with near unit probability,² while on Ge(100) the probability is dramatically smaller,^{3,4,5,6} on the order of 10⁻³ or less. Theoretical studies with a variety of methods^{1,7,8} show that the reaction on Si has little or no activation barrier. An analogous mechanism is expected on Ge, with its similar geometry and electronic structure, so it is somewhat surprising to find an apparent activation barrier on Ge. While there are many examples of unactivated reactions on Si(100) that are also unactivated on Ge(100), no simple analogy can predict the differences in water adsorption on the two surfaces.

In the following, we describe our understanding of this difference, on the basis of first-principles density functional theory calculations of the reaction path for dissociative adsorption of water on Ge(100). Some new features of the mechanism are revealed through a frontier orbital analysis derived from density functional theory (DFT) wave functions, clarifying the differences in reactivity of water on Si(100) and Ge(100). In the next section, we introduce the methods and models used. This is followed with the results of calculations of the bare surface, the reaction path, and the orbital analysis of the interactions at the transition state. We discuss these results, make further comparison to experiments, and conclude with a summary. Comparisons to analogous results on Si(100) are made throughout.

Theoretical Methods and Surface Model

The reaction path was calculated with a cluster model of the surface, consisting of 9 germanium atoms and 12 hydrogens (which replace subsurface germanium atoms). The top layer has

two Ge atoms, each with a dangling bond, thus modeling a single dimer of the (2 × 1) reconstructed surface. Cluster models of this type typically predict energies and geometries in good agreement with experiment, though there are some small systematic errors. Some of the differences are explored by using a larger cluster, Ge₂₁H₂₀, that models three adjacent dimers from a single dimer row.

The calculations reported here used the B3LYP hybrid density functional theory,⁹ as implemented in the *Gaussian98* suite of programs.¹⁰ All-electron geometry optimizations were done with the 6-31G** basis set. To compare single and multiple-dimer models, additional geometry optimizations were performed using the relativistic effective core potentials (RCEP) of Stevens, Basch, and Krauss.¹¹ The RCEP calculations used the CEP-121+G* basis, a split valence, triple- ζ basis with polarization and diffuse functions on the heavy atoms. Geometry optimizations were carried out without constraining any degrees of freedom. The matrix of second derivatives was calculated at each critical point to verify that it was a true minimum- or first-order saddle point. Minimizations were performed from the transition state to verify that it separates the expected reactant and product states.

Single-point energies and forces at the B3LYP/6-31G** critical point geometries were calculated with larger basis sets (up to 6-311++G(2df,2p)). In addition, a hybrid basis was used with 6-311++G(2df,2p) functions on the dimer atoms and the water molecule, while the 6-31G** basis was used on the subsurface atoms. We did not repeat the full optimization or frequency calculations with the larger bases. However, the force calculations verified that the geometry from the smaller basis still corresponded to a critical point on the potential surface for the larger bases. We also performed single-point calculations with the hybrid basis after small displacements from the transition state along the unstable normal mode to verify that the hybrid-basis potential energy surface had negative curvature in that direction.

Results

A. Clean Surface Structure. Prior work on Si(100) has shown that surface buckling plays a central role in dissociative adsorption mechanisms,^{1,7,8} and this is expected to be important on Ge(100) as well. In both cases, buckling creates surface states

* Corresponding author. E-mail: doren@udel.edu.

that can be viewed as mixtures of the π -like HOMO and π^* -like LUMO of the symmetric (unbuckled) dimer. This mixing not only lowers the energy of the HOMO, but can allow for better overlap of the surface and reactant orbitals. The buckled structure is much more stable on Ge(100) than on Si(100), so that the geometry is frozen at room temperature on Ge, while the Si dimers flip between different buckled states on a rapid time scale.

The optimal B3LYP/6-31G** geometry for the single-dimer model of Ge(100) has a buckling angle of 19.6° and a dimer bond length of 2.44 Å. This structure is 3.6 kcal/mol more stable than the optimal symmetric (C_{2v}) dimer. These values can be compared to a similar (BLYP/TZ94P) previous calculation for a Si(100) single-dimer model,¹ where the stabilization due to buckling is only 0.5 kcal/mol, with a buckling angle of 9.6° and a dimer bond length of 2.27 Å. Direct comparisons of Ge and Si single-dimer^{12,13} and periodic slab¹⁴ models using the same method and basis set have come to similar conclusions.

For Si(100), interdimer interactions cause greater buckling angles and stronger stabilization due to buckling.^{1,15} We have compared the buckling in single-dimer and three-dimer models of Ge(100) using the CEP-121+G* basis to optimize geometries for both. In the three-dimer model, adjacent dimers are buckled in opposite directions, giving the cluster a C_s symmetry plane through the central dimer. The central dimer is most strongly buckled (20.9°), and the average buckling angle for this three-dimer model is 20.5° ; both values are close to that of the single-dimer model (19.8°). The average energy difference per dimer (as calculated with the RECP basis) between the asymmetric three-dimer model and the symmetric one is 8 kcal/mol, as compared to the single-dimer model difference of 5.5 kcal/mol. Note that the stabilization energy, buckling angle and dimer bond length (2.48 Å) calculated for the single-dimer model with the RECP basis are all slightly greater than the values determined for the same model with the all-electron basis. Regardless of the basis or cluster model, all of these calculated values are in good agreement with experimentally determined geometry parameters, which range in value from 15.6° to 19.1° for the buckling angle and 2.44 to 2.55 Å for the dimer bond length.^{16–18}

One consequence of buckling is polarization of the electron distribution in the dimer. The single-dimer model of Ge(100) predicts natural atomic orbital charges¹⁹ of -0.22 e for the buckled-up dimer atom and $+0.14$ e for the buckled-down atom. Thus, buckling produces two chemically inequivalent sites, which will be reflected in the reactivity of the surface. For silicon, the electron-deficient, buckled-down atom reacts as an electrophile,^{1,20,21} while the buckled-up, electron-rich atom reacts as a weak nucleophile.^{22,23} Similar behavior is expected for germanium.

B. Reaction Pathway. A profile of the reaction path and the geometries associated with the critical points are shown in Figure 1. The geometric parameters of the critical points along the reaction coordinate (B3LYP/6-31G**) are given in Table 1; the relative energy differences between these points as calculated with several basis sets are given in Table 2. Energies are reported relative to the energy of the reactant state (isolated water molecule and Ge_9H_{12} cluster model). Note the strong basis set dependence (for fixed geometries) of the overall reaction energy and the activation energy for adsorption. In particular, the activation energy for adsorption varies over a range from -11.6 to $+7.4$ kcal/mol. The barrier for the reverse reaction (recombinative desorption) is much less sensitive to the basis set, varying over a range of only 2.5 kcal/mol. This pattern indicates

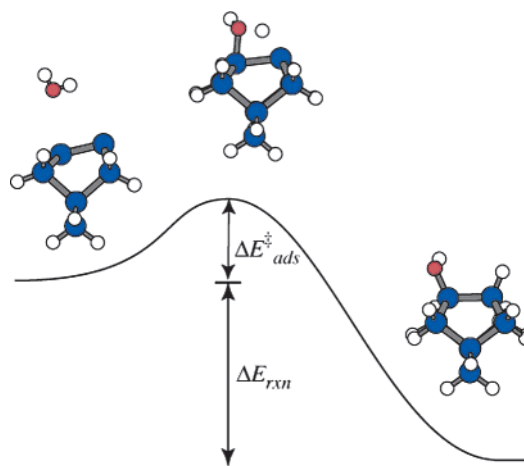


Figure 1. Reaction path for dissociative adsorption of water on a single-dimer cluster model of Ge(100). The structures shown were determined at the B3LYP/6-31G** level.

TABLE 1: Geometric Parameters for the Critical Points on the Reaction Path for Dissociative Adsorption of Water on Ge(100)-(2 × 1), as Calculated with B3LYP/6-31G^a**

	reactants		transition state		product	
	Ge	Si	Ge	Si	Ge	Si
$r(\text{X}-\text{X})$ (Å)	2.44	2.27	2.40	2.41	2.48	2.46
$r(\text{X}-\text{O})$ (Å)			1.95	1.94	1.81	1.76
$r(\text{O}-\text{H})$ (Å)	0.97	0.97	1.32	1.24		
	0.97	0.97	0.97	0.98	0.97	0.97
$r(\text{X}-\text{H})$ (Å)			1.84	1.95	1.53	1.50
dimer buckling (deg)	19.6	9.6	10.9	10.2	0.0	0.0

^a Earlier results (BLYP/TZ94P) for the analogous reaction on Si(100) are included for comparison. X = Si or Ge represents one of the dimer atoms.

TABLE 2: Basis Set Dependence of B3LYP Single-Point Energies (kcal/mol) at B3LYP/6-31G Critical Point Geometries^a**

basis	ΔE_{rxn}	$\Delta E_{\text{ads}}^{\ddagger}$	$\Delta E_{\text{des}}^{\ddagger}$
6-31G**	-52.9	-11.6	-41.3
6-311G**	-39.3	+1.5	-40.8
6-311++G	-44.2	-4.5	-39.7
6-311++G**	-33.7	+7.4	-41.1
6-311++G(2df,2p)	-36.2	+6.0	-42.2

^a The energy scale is set to zero for a separated water molecule and cluster model. The overall reaction energy and activation energy for dissociative adsorption are defined in Figure 1; the activation energy for recombinative desorption is $\Delta E_{\text{des}}^{\ddagger} = \Delta E_{\text{ads}}^{\ddagger} + \Delta E_{\text{rxn}}$.

that the isolated fragment reactant state is responsible for the variation, rather than the transition state. The range of values shown is dramatic, but all triple- ζ basis sets with polarization functions predict a positive activation barrier.

The transition state (TS) that separates the reactant state from the product state is predicted (via single-point calculations with the largest 6-311++G(2df,2p) basis at the 6-31G** optimized structures) to be higher in energy than the reactants by 6.0 kcal/mol (Table 2). Only one room-temperature molecule in 10^5 has enough energy to surmount a barrier of this magnitude, consistent with the low experimental sticking probability.

We have not included results for weakly bound precursor states, as there is some concern that DFT methods on small-cluster models cannot accurately predict their binding energies. Such states have no impact on equilibrium adsorption kinetics: assuming that the precursor state is in equilibrium with the separated reactants, the apparent activation energy depends only

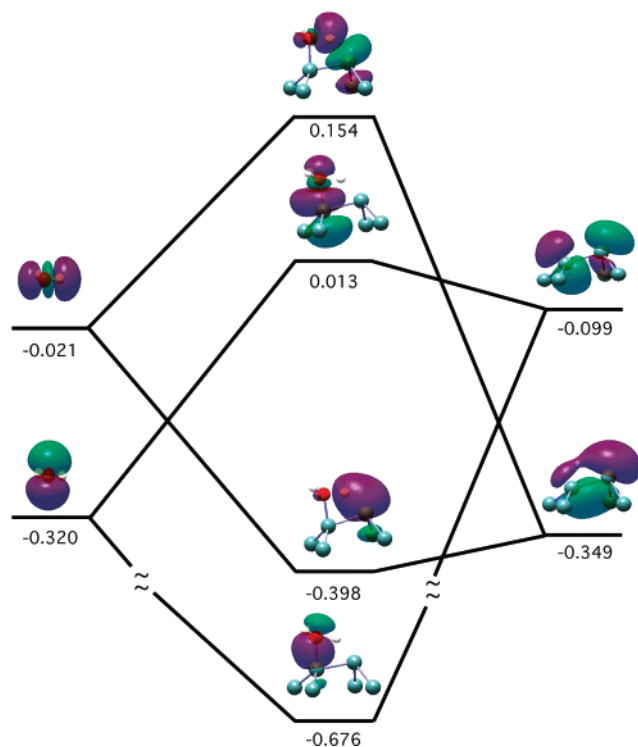


Figure 2. Frontier orbital diagram based on natural bond orbitals. Energies are in Hartrees.

on the difference in energy between the separated reactants and the transition state ($\Delta E_{\text{ads}}^{\ddagger}$).

The frequency of the unstable normal mode at the transition state is $1379i \text{ cm}^{-1}$. The orientation of the water molecule at the transition state is quite similar to that on Si, with the dissociating O–H bond lying in a plane that includes the dimer bond and the surface normal. The germanium dimer bond length at the TS structure has decreased slightly (0.04 \AA) relative to the bare surface. The buckling angle is 10.9° , some 8.6° less buckled than the bare surface dimer, bringing the dimer closer to the unbuckled product geometry. This change is in the opposite direction to the small increase observed on Si(100) (Table 1). Clearly, there is no simple association between increased buckling and enhanced reactivity.

The chemical interactions that determine the reaction path can be understood from a frontier orbital analysis of the DFT wave function. For systems of this size, the canonical orbitals are not generally helpful for such analysis: they are typically delocalized over the entire structure, and a single chemical bond may have contributions from a large number of orbitals. We have addressed this complication by using the natural bond orbitals (NBO's) developed by Weinhold and co-workers.¹⁹ The NBO's are a unitary transformation of the canonical orbitals that correspond to a Lewis structure description of the bonding. The resulting frontier orbitals for the reactants and the corresponding combinations at the transition state are shown in Figure 2.

The water molecule HOMO and LUMO are, respectively, an oxygen lone pair and an O–H antibonding orbital. The HOMO and LUMO of the surface are, respectively, the π -like and π^* -like dimer orbitals. This is the conventional description of the surface states, though the transition state NBO's are more readily described in terms of the individual dangling bond orbitals that compose the dimer HOMO and LUMO. At the transition state, the oxygen of the water molecule is positioned to allow the lone pair to interact with the electrophilic, buckled-

down side of the dimer bond. That is, the water HOMO overlaps with the surface dangling bond to form a nascent Ge–O bond at the transition state (the lowest energy orbital shown in Figure 2). Note the substantial decrease in the orbital energy associated with this interaction, putting this orbital in the same energy range as other substrate bonding orbitals. The NBO analysis identifies a single orbital that describes the dominant features of the Ge–O interaction.

Meanwhile, the O–H bond of the water molecule, which is coplanar with the dimer bond, is directed so that the positively charged hydrogen can interact with the nucleophilic, buckled-up side of the dimer. As previously reported on the Si surface, the surface-oxygen bond lengths at the transition state are close to their values in the final product (Table 1), consistent with substantial bond formation. However, fully formed Ge–O bonds are much weaker than Si–O bonds, and the partially formed Ge–O bond cannot stabilize the transition state as much as the corresponding silicon bond. Consequently, the Ge–O bond length at the TS is even closer to the product value (by 0.04 \AA) than the corresponding bond length on Si, and the dissociating O–H bond on Ge is longer than on Si. NBO analysis shows that the transition state wave function is well described as having no bond between the dissociating hydrogen and oxygen and a weak bond between the hydrogen and the nucleophilic (buckled-up) Ge atom on the far side of the dimer. The Ge–H bonding interaction provides some additional stabilization at the TS (Figure 2). This may be contrasted to the O–H bond in the TS on Si(100), which is 0.08 \AA shorter and appears to be intact in electron density analysis.¹ Calculations on isolated water molecules with the same geometries as in the two transition states show that at the Si(100) geometry, the water molecule is 20 kcal/mol above the minimum for isolated water, while at the Ge(100) geometry, it is 40 kcal/mol above the minimum.

Discussion

The transition state geometry for dissociation of water on Ge(100) is qualitatively similar to that on Si(100), but there are significant quantitative differences. The Ge dimer bond is less buckled, the Ge–O bond is closer to the product state value, and the O–H bond is longer than the corresponding value on Si. That is, the transition state on Ge is “later” (closer to the product state) than that on Si. Frontier orbital analysis shows that the dominant stabilizing interaction at the transition state is the formation of a bond between oxygen and a surface atom. The later transition state on Ge is a consequence of the weaker surface-oxygen bond that is not sufficient to stabilize an early transition state like that seen on Si. The transition state on Ge must lie closer to products before forces on the reaction coordinate favor motion toward products.

This kind of correlation among less endothermic reactions, later transition states, and higher activation barriers is often called the Hammond postulate in the context of organic chemistry. While this may be useful in surface reactions as a post hoc interpretation of differences in activation energy, it is clearly not useful as a predictive tool. For example, the [4+2] cycloaddition reaction of conjugated dienes also has a much weaker thermodynamic driving force on Ge^{24,25} than on Si,^{26,27} yet the reaction appears to be unactivated on both surfaces.

Quite recently, another study of water on Ge(100) has been reported using a different density functional with periodic slab models and a plane-wave basis.²⁸ These authors find a similar activation barrier to that shown here. Even allowing for the differences in functionals, basis sets, and geometry search methods, it is clear that there are no dramatic differences

between the results of calculations using cluster models and periodic models of the surface. Both types of model have their flaws: clusters neglect interactions with more distant surface sites, while periodic slab methods treat chemical reactions as though they had spatial periodicity. The fact that both methods draw similar conclusions indicates that (in the present case) the errors due to either model are likely to be small.

Finally, we note that several experimental studies have shown that water can be efficiently dissociated on Ge(100) by adsorbing (nondissociatively) at low temperature (e.g., liquid nitrogen temperature), and then heating the surface to room temperature.^{3,4,5} These experiments demonstrate the existence of a molecular precursor state on the surface that we have not explored here. Molecules that have been adsorbed to the surface at low temperature can either desorb or dissociate on heating. The relative rates of these processes depend on the difference in the corresponding free energies of activation. The fact that the direct sticking probability is small at room temperature implies that there is a free energy barrier to dissociation that is higher than the free energy of separated reactants, at least at low coverage. Thus, in the absence of interadsorbate interactions, molecules in a precursor state would be much more likely to desorb than to dissociate. This low coverage situation corresponds to the model studied in our work, and our prediction of the transition state energy in this situation implies that desorption from the precursor should be strongly favored over dissociation in this case. On the other hand, if a layer of water is deposited at low temperature, it will have strong intermolecular interactions. These can change the reaction path substantially, and the experimental observation that dissociation occurs on heating an adsorbed layer implies that interadsorbate interactions disfavor desorption relative to dissociation.

Summary

The dramatic difference in dissociative sticking probability of water on Si(100) and Ge(100) has been reproduced in density functional theory calculations on cluster models of the surface. This difference in reactivity is too subtle to predict by qualitative arguments, so it is essential to have predictive methods capable of distinguishing such cases. DFT with cluster models appears to be capable of drawing such distinctions. However, some care must be exercised with basis sets, even to obtain qualitatively correct results in this case. Natural bond orbital analysis shows that the transition state is stabilized by Ge—O and (to a lesser degree) Ge—H interactions. The primary difference from silicon

is the weaker Ge—O bond, which does not draw the system toward the dissociated state as effectively as the stronger bond on Si.

References and Notes

- (1) Konecny, R.; Doren, D. J. *J. Chem. Phys.* **1997**, *106*, 2426.
- (2) (a) Chabal, Y. J.; Christman, S. B. *Phys. Rev. B* **1984**, *29*, 6974. (b) Chabal, Y. J. *J. Vac. Sci. Technol. A* **1985**, *3*, 1448.
- (3) Kuhr, H. J.; Ranke, W. *Surf. Sci.* **1987**, *187*, 98.
- (4) (a) Papagno, L.; Caputi, L. S.; Frankel, D.; Chen, Y.; Lapeyre, G. *J. Surf. Sci.* **1987**, *189/190*, 199. (b) Papagno, L.; Frankel, D.; Chen, Y.; Caputi, L. S.; Anderson, J.; Lapeyre, G. *J. Surf. Sci.* **1991**, *248*, 343.
- (5) (a) Larsson, C. U. S.; Flödstrom, A. S.; Karlsson, Y.; Yang, Y. *J. Vac. Sci. Technol. A* **1989**, *7*, 2044. (b) Larsson, C. U. S.; Flödstrom, A. S. *Vacuum* **42**, 297.
- (6) Cohen, S. M.; Yang, Y.; Rouchouze, E.; Jin, T.; D'Evelyn, M. P. *J. Vac. Sci. Technol. A* **1992**, *10*, 2166.
- (7) Cho, J.-H.; Kim, K. S.; Lee, S.-H.; Kang, M.-H. *Phys. Rev. B* **2000**, *61*, 4503.
- (8) Jung, Y.; Choi, C. H.; Gordon, M. S. *J. Phys. Chem. B* **2001**, *105*, 4039.
- (9) (a) Lee, C.; Yang, W.; Parr, R. G. *Phys. Rev. B* **1988**, *37*, 785. (b) Becke, A. D. *J. Chem. Phys.* **1993**, *98*, 5648.
- (10) Frisch, M. J.; et al. *Gaussian 98*, Revision A.9; Gaussian Inc.: Pittsburgh, PA, 1998.
- (11) Stevens, W. J.; Krauss, M.; Basch, H. *Can. J. Chem.* **1992**, *70*, 612.
- (12) Hess, J. S.; Doren, D. J. *J. Chem. Phys.* **2000**, *113*, 9353.
- (13) Yang, C.; Kang, H. C. *J. Chem. Phys.* **1999**, *110*, 11029.
- (14) Krüger, P.; Pollmann, J. *Phys. Rev. Lett.* **1995**, *74*, 1155.
- (15) Penev, E.; Kratzer, P.; Scheffler, M. *J. Chem. Phys.* **1999**, *110*, 3986.
- (16) Rossman, R.; Meyerheim, H. L.; Jahns, V.; Wever, J.; Moritz, W.; Wolf, D.; Dornisch, D.; Schulz, H. *Surf. Sci.* **1992**, *279*, 199.
- (17) Ferrer, S.; Torrelles, X.; Etgens, V. H.; van der Vegt, H. A.; Fajardo, P. *Phys. Rev. Lett.* **1995**, *75*, 1771.
- (18) Torrelles, X.; van der Vegt, H. A.; Etgens, V. H.; Fajardo, P.; Alvarez, J.; Ferrer, S. *Surf. Sci.* **1996**, *364*, 242.
- (19) Glendening, E. D.; Badenhoop, J. K.; Reed, A. E.; Carpenter, J. E.; Weinhold, F. A. *NBO 5.0*; Theoretical Chemistry Institute, University of Wisconsin: Madison, WI, 1998.
- (20) Fattal, E.; Radeke, M. K.; Reynolds, G.; Carter, E. A. *J. Phys. Chem. B* **1997**, *101*, 8658.
- (21) Widjaja, Y.; Mysinger, M. M.; Musgrave, C. B. *J. Phys. Chem. B* **2000**, *104*, 2527.
- (22) Robinson Brown, A.; Doren, D. J. *J. Chem. Phys.* **1999**, *110*, 2643.
- (23) Konecny, R.; Doren, D. J. *J. Phys. Chem.* **1997**, *101*, 10983.
- (24) Teplyakov, A. V.; Lal, P.; Noah, Y. A.; Bent, S. F. *J. Am. Chem. Soc.* **1998**, *120*, 7377.
- (25) Föraker, A.; Doren, D. J. Unpublished results.
- (26) Konecny, R.; Doren, D. J. *J. Am. Chem. Soc.* **1997**, *119*, 11098.
- (27) Teplyakov, A. V.; Kong, M. J.; Bent, S. F. *J. Am. Chem. Soc.* **1997**, *119*, 11100.
- (28) Cho, J. H.; Kleinman, L.; K. Jin; Kim, K. S.; *Phys. Rev. B* **2002**, *66*, 113306.